

## Supporting Information

### **Intrinsic ferroelastic valleytronics in 2D Pd<sub>4</sub>X<sub>3</sub>Te<sub>3</sub> (X = S, Se) materials: a new platform for ultrafast intervalley carrier dynamics**

Chengan Lei <sup>a</sup>, Zhao Qian <sup>a,\*</sup>, Yandong Ma <sup>b</sup>, Rajeev Ahuja <sup>c</sup>

<sup>a</sup> *Key Laboratory for Liquid-Solid Structural Evolution and Processing of Materials (Ministry of Education), State Key Laboratory of Advanced Equipment and Technology for Metal Forming, Shandong University, Jinan 250061, China*

<sup>b</sup> *School of Physics, State Key Laboratory of Crystal Materials, Shandong University, Jinan 250100, China*

<sup>c</sup> *Condensed Matter Theory, Materials Theory Division, Department of Physics and Astronomy, The Ångström Laboratory, Uppsala University, Uppsala 75120, Sweden*

*\*Correspondence to: qianzhao@sdu.edu.cn*

## Computational details

### 1. Real-Time Time-Dependent Density Functional Theory in the Kohn-Sham Formulation

Time-dependent (TD) Kohn-Sham (KS) equation

$$i\hbar \frac{\partial}{\partial t} \Psi(\mathbf{r}, t) = \hat{H}(\mathbf{r}, \mathbf{R}) \Psi(\mathbf{r}, t). \quad (1)$$

We can expand the wavefunction  $\Psi(\mathbf{r}, t)$  in a basis,  $\Phi(\mathbf{r}; \mathbf{R}(t))$ .

$$\Psi_j(\mathbf{r}, t) = \sum_k C_k^j(t) \Phi_k(\mathbf{r}; \mathbf{R}(t)) \quad (2)$$

$\Psi(\mathbf{r}, t)$  is TDKS orbitals, and  $\Phi(\mathbf{r}; \mathbf{R}(t))$  is the ground-state KS orbital. Substituting the equation (2) into the equation (1) gives

$$i\hbar \frac{\partial}{\partial t} C_k^j(t) = \sum_m C_m^j(t) \left( \dot{\phi}_m \delta_{km} - i\hbar \mathbf{d}_{km} \cdot \dot{\mathbf{R}} \right) \quad (3)$$

where nonadiabatic coupling vector

$$\mathbf{d}_{km} = \langle \phi_k(\mathbf{r}; \mathbf{R}) | \nabla_{\mathbf{R}} | \phi_m(\mathbf{r}; \mathbf{R}) \rangle. \quad (4)$$

### 2. The Autocorrelation Function, Spectral Density and Decoherence Time

First, the autocorrelation function (ACF)

$$C_{ij}(t) = \frac{\langle \delta E_{ij}(t') \delta E_{ij}(t-t') \rangle_{t'}}{\langle \delta E_{ij}^2(0) \rangle} = \frac{C_{\text{un}}(t)}{\langle \delta E_{ij}^2(0) \rangle} \quad (5)$$

where  $\delta E_{ij}(t) = \Delta E_{ij}(t) - \langle \Delta E_{ij}(t) \rangle$ . The  $C_{\text{un}}(t)$  and  $\Delta E_{ij}(t)$  are the unnormalized ACF and energy gap between electronic states  $i$  and  $j$ , respectively.

Then, the spectral density is obtained through the Fourier transform of ACF

$$I(\omega) = \left| \frac{1}{\sqrt{2\pi}} \int_{-\infty}^{+\infty} dt e^{-i\omega t} C_{ij}(t) \right|^2. \quad (6)$$

It can identify which frequencies of phonon vibrations are coupled with the electronic degrees of freedom. Meanwhile, the amplitude of the phonon vibration mode reflects the intensity of the phonon mode of the electron-phonon coupling at a given frequency.

Finally, the decoherence function is calculated as

$$D_{ij}(t) = \exp \left( -\frac{1}{\hbar^2} \int_0^t dt' \int_0^{t'} dt'' C_{ij}(t'') \right). \quad (7)$$

By fitting the decoherence function to a Gaussian model, we can extract the characteristic decoherence timescale.

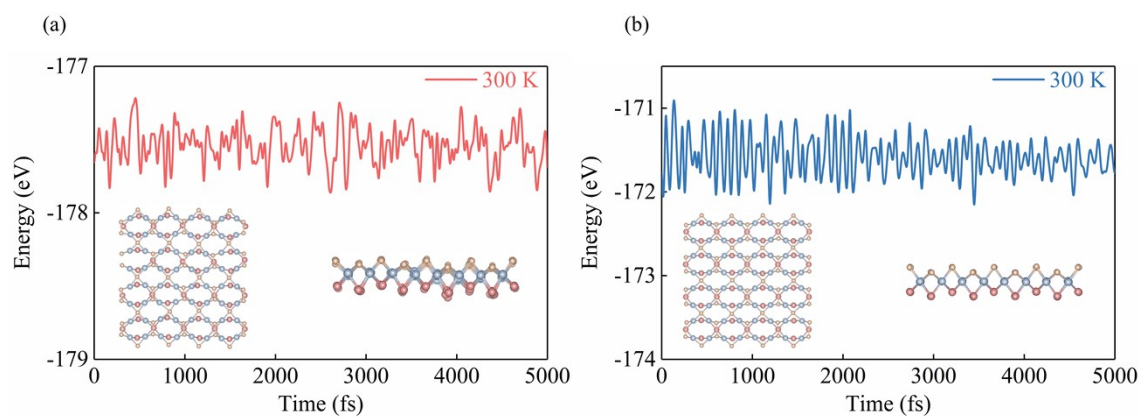


**Figure S1.** Variation of the total energy of (a)  $\text{Pd}_4\text{S}_3\text{Te}_3$  and (b)  $\text{Pd}_4\text{Se}_3\text{Te}_3$  with time obtained from AIMD simulation at 300 K. Insets in (a) and (b) are the snapshots taken from the end of the AIMD simulations.

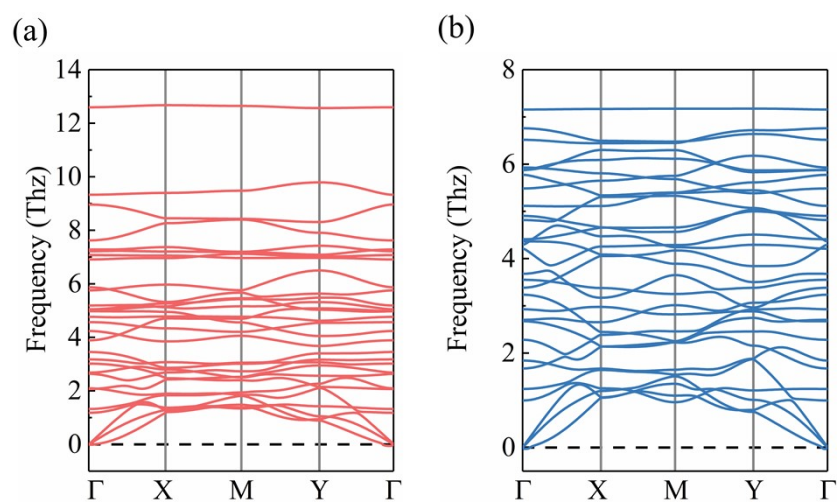


**Figure S2.** Phonon spectra of (a)  $\text{Pd}_4\text{S}_3\text{Te}_3$  and (b)  $\text{Pd}_4\text{Se}_3\text{Te}_3$ .

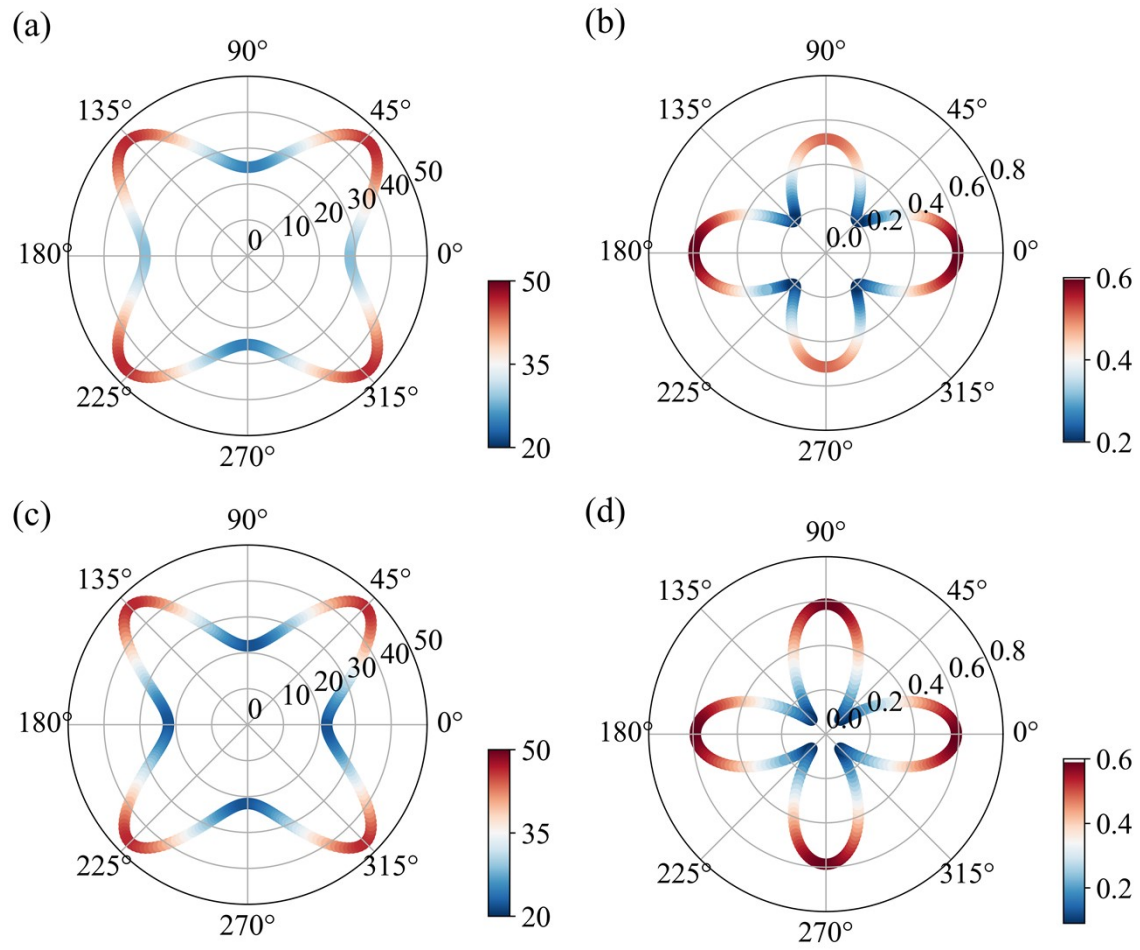


**Figure S3.** (a) Young's modulus, (b) Poisson's ratio of  $\text{Pd}_4\text{S}_3\text{Te}_3$ , (c) Young's modulus and (d) Poisson's ratio of  $\text{Pd}_4\text{Se}_3\text{Te}_3$  as a function of the angle  $\theta$  ( $\theta = 0^\circ$  corresponds to the  $x$  axis).

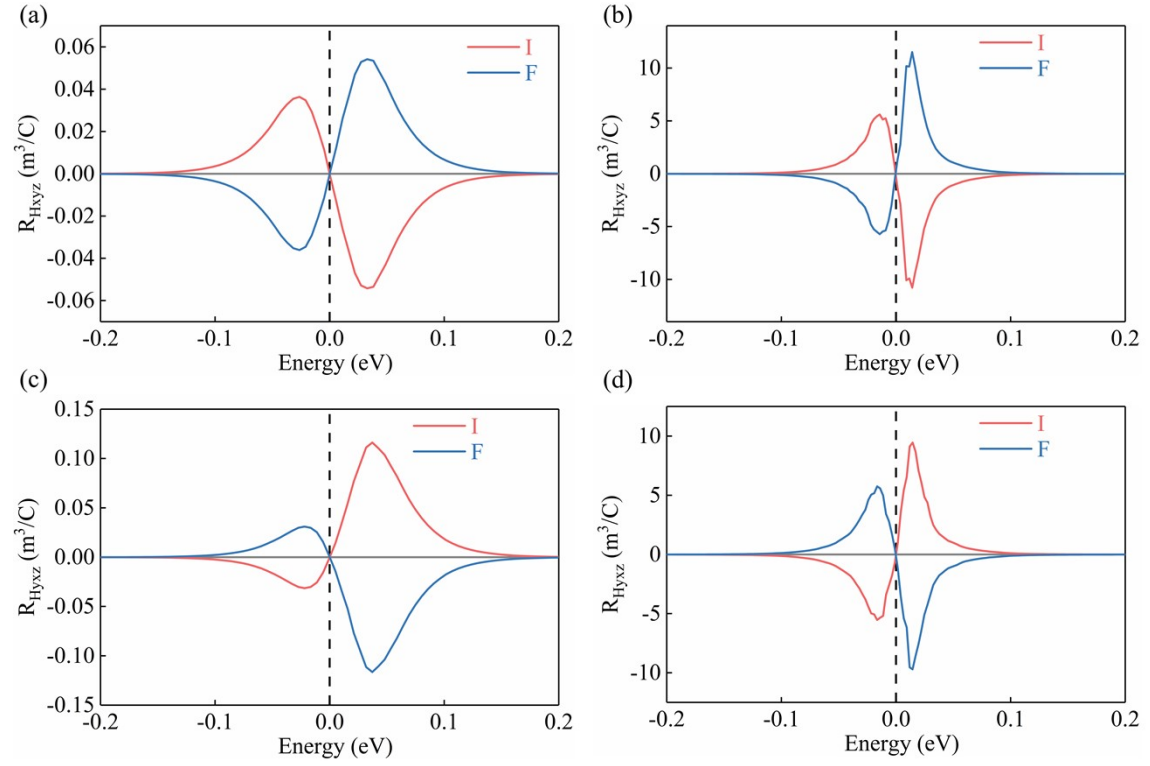


**Figure S4.** Simulated room temperature Hall coefficient  $R_{Hxyz}$  as a function of chemical potential for I and F states of (a)  $\text{Pd}_4\text{S}_3\text{Te}_3$  and (b)  $\text{Pd}_4\text{Se}_3\text{Te}_3$ . Simulated room temperature Hall coefficient  $R_{Hxyz}$  as a function of chemical potential for I and F states of (c)  $\text{Pd}_4\text{S}_3\text{Te}_3$  and (d)  $\text{Pd}_4\text{Se}_3\text{Te}_3$ .

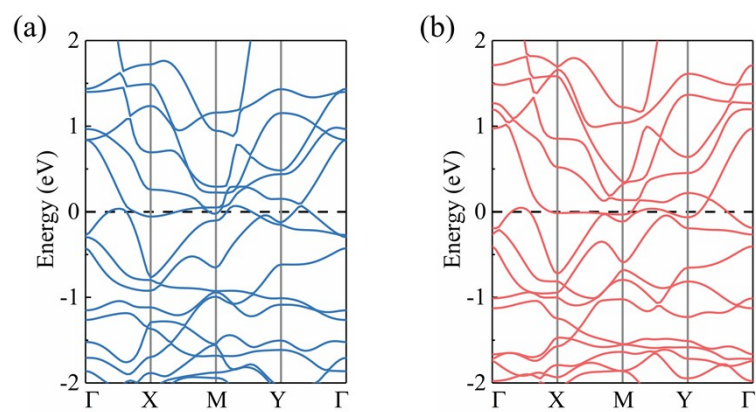


**Figure S5.** Simulated band structures for paraelastic phase (a)  $\text{Pd}_4\text{S}_3\text{Te}_3$  and (b)  $\text{Pd}_4\text{Se}_3\text{Te}_3$ .

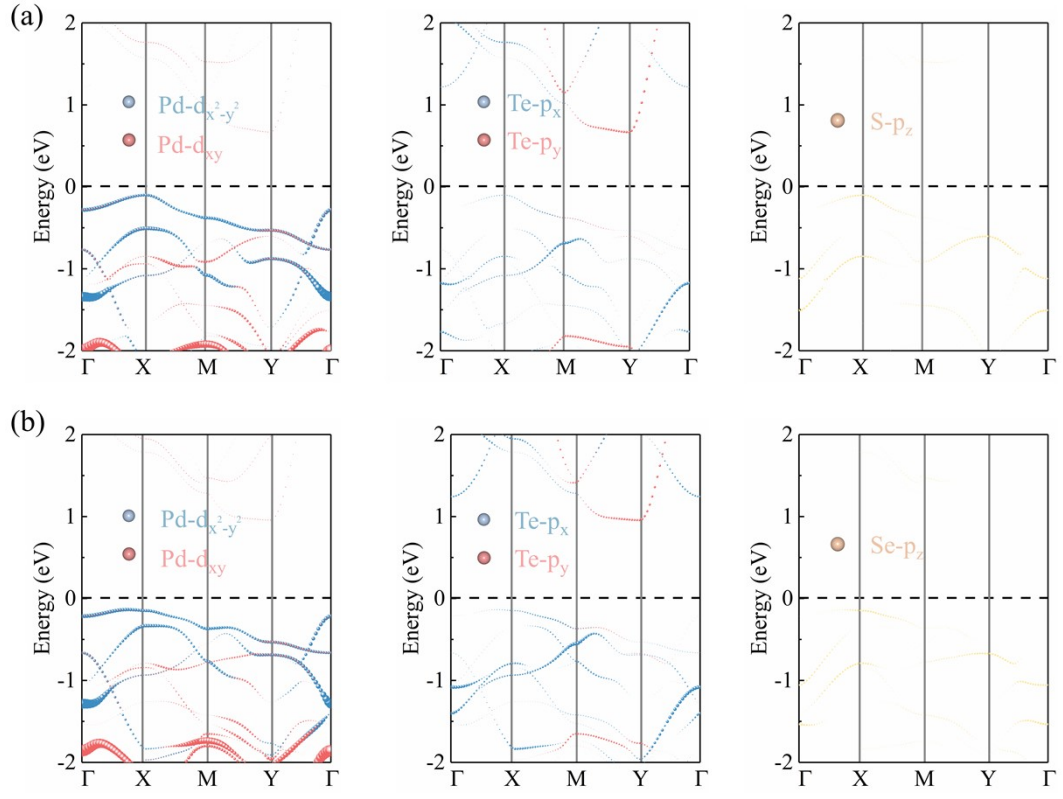


**Figure S6.** Simulated orbital-resolved band structures for (a)  $\text{Pd}_4\text{S}_3\text{Te}_3$  and (b)  $\text{Pd}_4\text{Se}_3\text{Te}_3$ .